nature publishing group

Basic Science Investigation | Articles

Optimal mean airway pressure during high-frequency oscillatory ventilation determined by measurement of respiratory system reactance

Emanuela Zannin[1], Maria Luisa Ventura[2], Raffaele L. Dellacà[1], Miria Natile[2], Paolo Tagliabue[2], Elizabeth J. Perkins[3,4], Magdy Sourial[4], Risha Bhatia[3], Peter A. Dargaville[3,5,6] and David G. Tingay[3,4,7]

BACKGROUND: The aims of the present study were (i) to characterize the relationship between mean airway pressure (P_{AW}) and reactance measured at 5 Hz (reactance of the respiratory system (X_{RS}), forced oscillation technique) and (ii) to compare optimal P_{AW} (P_{opt}) defined by X_{RS}, oxygenation, lung volume (V_L), and tidal volume (V_T) in preterm lambs receiving high-frequency oscillatory ventilation (HFOV).

METHODS: Nine 132-d gestation lambs were commenced on HFOV at P_{AW} of 14 cmH$_2$O (P_{start}). P_{AW} was increased stepwise to a maximum pressure (P_{max}) and subsequently sequentially decreased to the closing pressure (P_{cl}, oxygenation deteriorated) or a minimum of 6 cmH$_2$O, using an oxygenation-based recruitment maneuver. X_{RS}, regional V_L (electrical impedance tomography), and V_T were measured immediately after (t_{0min}) and 2 min after (t_{2min}) each P_{AW} decrement. P_{opt} defined by oxygenation, X_{RS}, V_L, and V_T were determined.

RESULTS: The P_{AW}–X_{RS} and P_{AW}–V_T relationships were dome shaped with a maximum at P_{cl}+6 cmH$_2$O, the same point as P_{opt} defined by V_L. Below P_{cl}+6 cmH$_2$O, X_{RS} became unstable between t_{0min} and t_{2min} and was associated with derecruitment in the dependent lung. P_{opt}, as defined by oxygenation, was lower than the P_{opt} defined by X_{RS}, V_L, or V_T.

CONCLUSION: X_{RS} has the potential as a bedside tool for optimizing P_{AW} during HFOV.

High-frequency oscillatory ventilation (HFOV) is used to treat severe neonatal lung disease and has the potential to reduce ventilator-induced lung injury when applied optimally (1,2). HFOV optimally applied aims to recruit the lung and subsequently reduce mean airway pressure (P_{AW}) to an optimal pressure (P_{opt}) that achieves optimal lung recruitment at the lowest distending pressure (open lung strategy) (3,4). However, identification and maintenance of P_{opt} remains challenging, particularly in the newly born, whose lungs are in a highly dynamic state because of fluid reabsorption and establishment of functional residual capacity (5). The lack of appropriate tools for the bedside assessment and continuous monitoring of lung function in infants makes targeting of P_{opt} even more difficult.

Oxygenation, evaluated by monitoring oxygen saturation (Sp_{O2}), is most commonly used for targeting P_{opt} during HFOV in clinical practice (6). However, Sp_{O2} is an imperfect guide for P_{AW} titration as it is relatively uniform over a wide range of airway pressures and volumes (7). Beginning with the observations of Suter *et al.* (8), the notion that lung mechanics can guide pressure settings during mechanical ventilation has been examined carefully. For conventional ventilation, a relationship between end-expiratory lung volume (V_L), recruitment, and tidal breath mechanics has been demonstrated repeatedly (9,10). During HFOV, the same theoretical considerations apply (3), but the best means of assessing the mechanics of the oscillated lung remains unclear.

A promising approach to noninvasive bedside assessment of lung mechanics in ventilated newborns is the forced oscillation technique (FOT) (11–14). FOT measures the mechanical impedance of the respiratory system (Z_{RS}) by evaluating its response to pressure oscillations (15). Z_{RS} is commonly expressed in terms of resistance of the expiratory system (R_{RS}) and reactance of the respiratory system (X_{RS}), which in turn represents the elastic and inertive properties of the system. Recent studies, using broad-band stimulating signals including very-low-frequency components (low frequency forced oscillation technique (LFOT)), showed that the frequency dependence of R_{RS} is a sensitive indicator of mechanical heterogeneities in the lungs and that low-frequency dynamic elastance can be used to assess V_L recruitment and distention during ventilation (16–20). Moreover, if proper mathematical interpretative models are applied to LFOT data, it is possible to discriminate between the mechanical properties of airways and lung tissue. This approach identified hysteresivity as the most sensitive parameter to V_L recruitment in the preterm

[1]Dipartimento di Elettronica Informazione e Bioingegneria, Politecnico di Milano University, Milano, Italy; [2]Neonatology and Neonatal Intensive Care Unit, Fondazione MBBM - Ospedale San Gerardo, Monza, Italy; [3]Neonatal Research, Murdoch Childrens Research Institute, Melbourne, Victoria, Australia; [4]Department of Neonatology, Royal Children's Hospital, Melbourne, Victoria, Australia; [5]Department of Paediatrics, Royal Hobart Hospital and University of Tasmania, Hobart, Tasmania, Australia; [6]Neonatal Respiratory Group, Menzies Research Institute, Hobart, Tasmania, Australia; [7]Department of Paediatrics, University of Melbourne, Melbourne, Victoria, Australia. Correspondence: Emanuela Zannin (emanuela.zannin@polimi.it)

Received 8 July 2013; accepted 24 September 2013; advance online publication 29 January 2014. doi:10.1038/pr.2013.251

lung (21). Unfortunately, clinical application of LFOT for continuous bedside monitoring is limited by its high sensitivity to leaks and, importantly, by the interference of spontaneous breathing on the low-frequency components of the forcing signal. Recently, single-frequency FOT has been applied during conventional mechanical ventilation both in animal models (17,20,22,23) and in ventilated preterm newborns (11). In particular, X_{RS} at 5 Hz (X_{RS}) identified the lowest positive end-expiratory pressure level able to keep the lung fully recruited (22,23), minimizing lung injury (23). Moreover, it has been demonstrated that changes in X_{RS} measured at 5 Hz can also be evaluated during HFOV from the high-amplitude oscillatory waveform delivered by the ventilator allowing, in principle, FOT measurement without suspending the delivery of ventilation to the patient (24).

We hypothesized that monitoring the dynamics of X_{RS} during decremental pressure steps on HFOV, after recruitment, would allow the identification of approaching derecruitment without waiting for physiological variables with long stabilization times, and without bringing the lung to significant derecruitment to identify the lowest P_{AW} able to prevent atelectasis. Based on this hypothesis, we evaluated the temporal change in X_{RS} at each step during a trial of decreasing P_{AW} after volume recruitment. P_{opt} was defined as the lowest P_{AW} at which X_{RS} does not decrease over time within a P_{AW} step. We reasoned that P_{opt} thus defined should maintain recruitment and stability of lung mechanics.

The aims of this study were (i) to characterize the relationships between X_{RS}, measured while delivering HFOV, and pressure, oxygenation, regional V_Ls, and tidal volume (V_T) and (ii) to compare P_{opt} defined by X_{RS} with that defined by oxygenation, V_L, or V_T, during a trial of decreasing P_{AW} after volume recruitment.

RESULTS

Animal Characteristics

Nine lambs (six male) with a mean (SD) birth weight of 3.5 (0.9) kg and cord pH immediately prior to birth of 7.38 (0.03) were studied. All animals completed the protocol without complications, including no evidence of pneumothorax. **Table 1** reports ventilator settings, arterial blood gas, and hemodynamic variables at relevant protocol steps. After attaining P_{max}, gas exchange improved markedly, whereas mean arterial pressure and heart rate decreased. As P_{AW} was reduced, blood pressure and heart rate were restored. Changing oscillatory frequency to 5 Hz for the duration of FOT measurements did not modify V_L.

Relationship Between X_{RS} and Other Variables

Figure 1 shows the relationships of oxygenation, X_{RS}, V_L, and V_T with P_{AW} during mapping of the deflation limb in a representative animal. As P_{AW} was reduced from P_{max} to 12 cmH_2O, the lung displayed a predominantly elastic behavior: X_{RS} increased (became less negative, indicating an increase in respiratory system compliance), suggesting a reduction in tissue distension. For pressure values lower than 12 cmH_2O, there was no subsequent sustained benefit in X_{RS}, and a noticeable reduction between t_{0min} and t_{2min} occurred with subsequent steps, suggesting that the applied pressure was no longer able to maintain recruitment. Therefore, for the subject shown, P_{opt} defined by X_{RS} was 12 cmH_2O. This was also the upper corner pressure (P_{opt} value) of the P_{AW}–V_L relationship. In contrast, oxygenation was unchanged between P_{max} and a P_{AW} of 10 cmH_2O and then decreased rapidly as P_{AW} was reduced further, resulting in an oxygenation-defined P_{opt} of 10 cmH_2O. Finally, the P_{AW}–V_T relationship was dome shaped with maximum V_T (P_{opt}) occurring at 14 cmH_2O.

Table 1. Ventilatory and physiological indices at selected protocol steps

	P_{start}	P_{max}	P_{cl}
P_{AW} (cmH_2O)	14.0 (0.0)*	28.2 (1.5)	10.7 (2.0)*
Amplitude (cmH_2O)	45.6 (5.3)	46.7 (6.1)	46.1 (7.0)
FiO_2	0.6 (0.4)	0.3 (0.3)	0.3 (0.2)
P_{O2} (mmHg)	31.5 (6.0)	47.3 (5.2)	29.6 (2.7)*
OI	58.0 (23.0)*	19.8 (7.2)	10.9 (3.7)*
a/A	0.26 (0.08)*	0.48 (0.06)	0.32 (0.05)
P_{CO2} (mm Hg)	60.4 (7.1)	50.8 (3.9)	52.7 (4.5)
MAP (mmHg)	48.6 (5.3)*	34.9 (4.6)	49.0 (4.2)*
HR (bpm)	150.4 (12.3)	138.1 (11.0)	149.0 (9.0)

Data reported as mean (SEM).
a/A, arterial/alveolar oxygen tension ratio; HR, heart rate; MAP, mean arterial pressure; OI, oxygenation index; P_{AW}, mean airway pressure; P_{cl}, closing pressure; P_{max}, maximum pressure; P_{start}, initial pressure; P_{O2}, partial pressure of oxygen; P_{CO2}, partial pressure of carbon dioxide.
*$P < 0.05$ vs. P_{max} (one-way ANOVA for repeated measurements, with Tukey *post hoc* test).

Combining data from all animals, P_{max} occurred on average (SD) at 28.2 (4.5) cmH_2O (**Figure 2**). Attaining P_{max} resulted in a marked improvement in oxygenation, lung mechanics, V_L, and V_T compared with P_{start} (**Table 2**). Thereafter, on the deflation limb, P_{cl} occurred at 10.7 (5.9) cmH_2O.

Overall, oxygenation remained stable until P_{cl}+2 cmH_2O. At 2 min, the average P_{AW}–X_{RS} relationship presented a maximum at P_{cl}+6 cmH_2O. At pressures below P_{cl}+6 cmH_2O, X_{RS} decreased between t_{0min} and t_{2min}, indicating that V_L recruitment could not be maintained. The X_{RS}-defined P_{opt} of P_{cl}+6 cmH_2O also coincided with the upper corner pressure of the P_{AW}–V_L relationship and with the maximum of the P_{AW}–V_T relationship, indicating a common P_{opt} value. In addition, below P_{cl}+6 cmH_2O, both V_L and V_T were unstable between t_{0min} and t_{2min}, suggesting that this was the P_{AW} value in which derecruitment became significant within the lung. The regional V_L data supported this. Below P_{cl}+6 cmH_2O, the dorsal hemithorax demonstrated a greater change in V_L than the ventral hemithorax, suggesting a nonuniform gravity-dependent pattern of derecruitment (**Figure 3**).

P_{opt} Defined by Oxygenation, X_{RS}, V_L, and V_T

In all subjects, oxygenation defined a significantly lower P_{opt} than reactance, V_L, and V_T. Mean (95% confidence interval) P_{opt} defined by oxygenation was 4.4 (1.9, 7.0) cmH_2O lower than the P_{opt} defined by X_{RS}, 4.5 (2.5, 6.5) cmH_2O lower than V_L-defined P_{opt}, and 3.6 (2.1, 5.1) cmH_2O lower than V_T-defined P_{opt}. Oxygenation was not different between the P_{opt} for

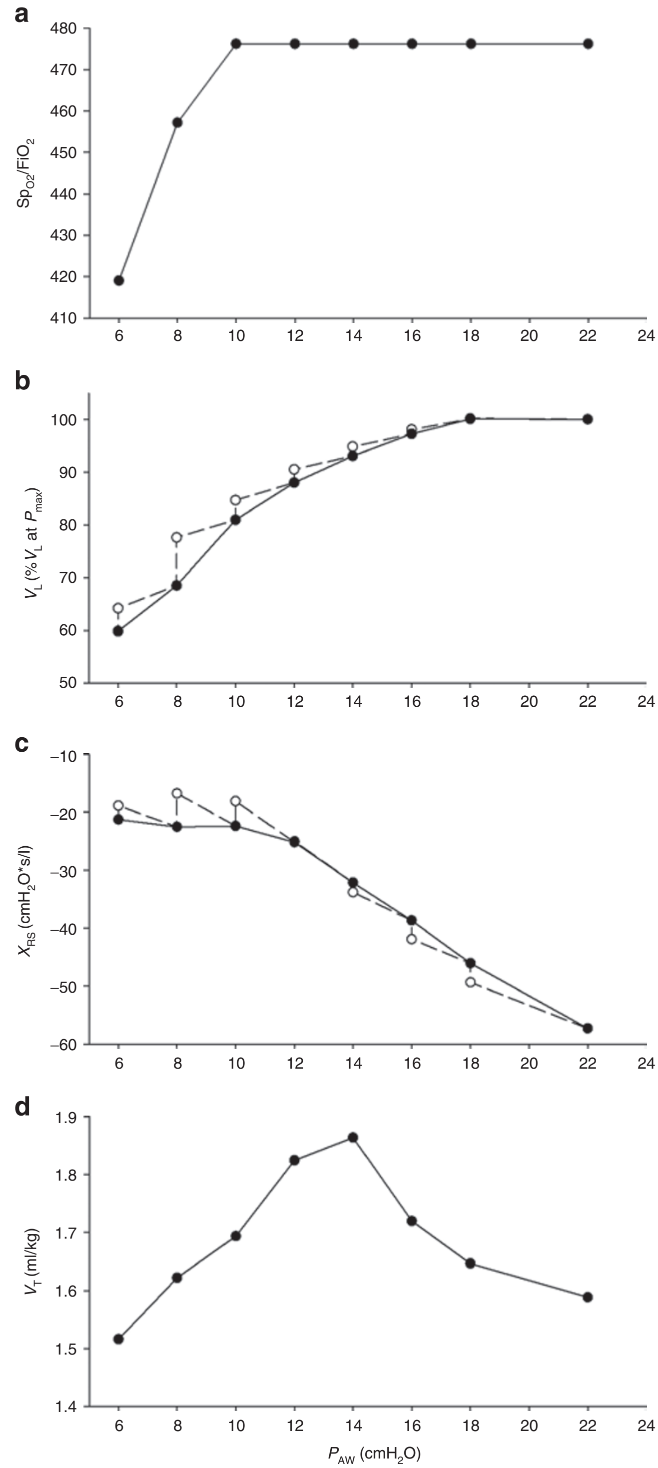

Figure 1. Relationship between pressure and relevant variables in a representative animal. Relationship between mean airway pressure (P_{AW}) and (**a**) oxygenation (Sp$_{O2}$/FiO$_2$), (**b**) lung volume (V_L), (**c**) reactance of the respiratory system (X_{RS}), and (**d**) tidal volume (V_T) during the deflation series in a representative animal. Change in V_L and X_{RS} values immediately after (t_{0min}; open circles) and 2 min after (t_{2min}; closed circles) each P_{AW} decrement are also shown.

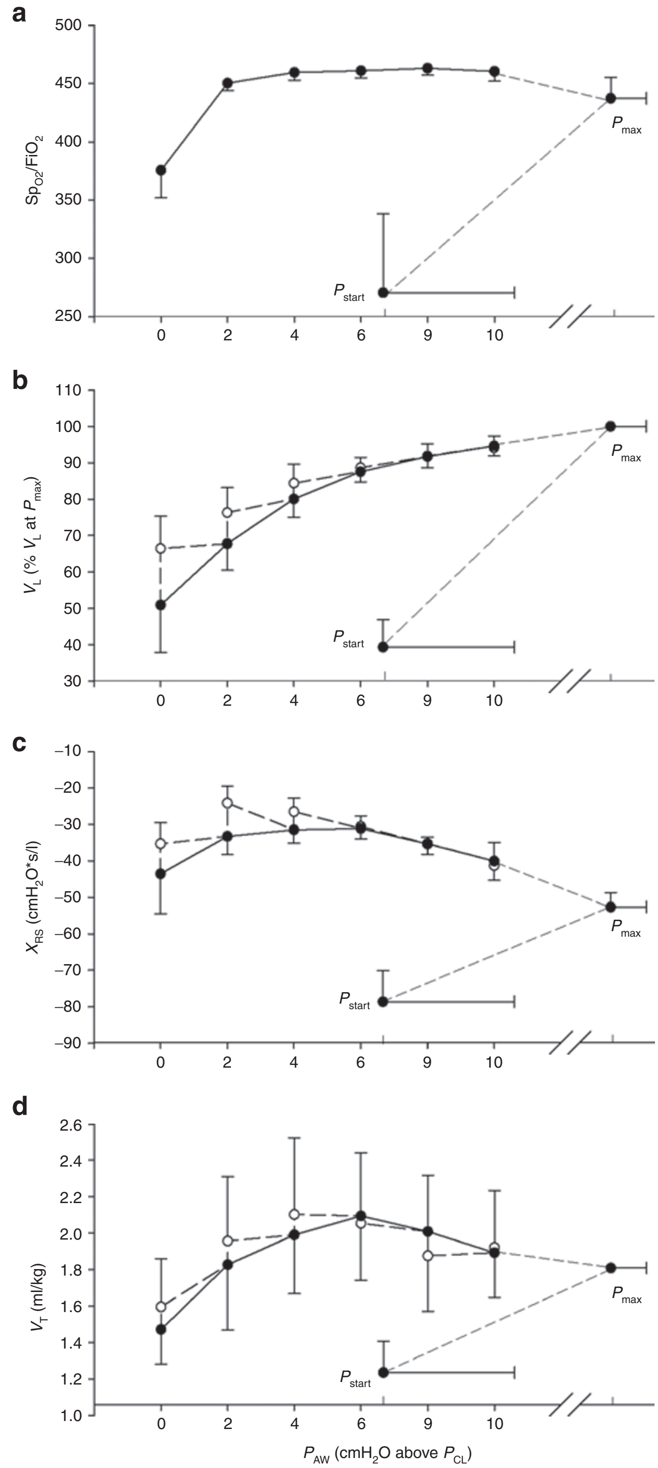

Figure 2. Mean relationship between pressure and relevant variables. Relationship between mean airway pressure (P_{AW}) at key steps in the mapping of the pressure–volume relationship and (**a**) Sp$_{O2}$/FiO$_2$, (**b**) lung volume (V_L), (**c**) reactance of the respiratory system (X_{RS}), and (**d**) tidal volume (V_T). In each figure, data for initial pressure (P_{start}), maximum pressure (P_{max}), and five decremental P_{AW} series before closing pressure (P_{cl}) are shown. V_L is expressed as a percentage of the V_L at P_{max}. The X_{RS} and V_L data at t_{0min} (solid lines, closed circles) and t_{2min} (open circles, dotted lines) of each P_{AW} step are shown. Optimal pressure (P_{opt}) defined by oxygenation occurred at P_{cl}+2 cmH$_2$O, whereas X_{RS}, V_L, and V_T identified a P_{opt} at P_{cl}+6 cmH$_2$O, and the point of sign change in the t_{0min} to t_{2min} relationship for each parameter. All data are expressed as mean and SEM. Sp$_{O2}$, oxygen saturation.

Table 2. Changes in oxygenation, reactance, V_L, and V_T attaining maximal recruitment

	P_{start}	P_{max}
Spo_2/FiO_2	249 (67)	413 (30)*
X_{RS} (cmH_2O*s/l)	−84 (9)	−53 (4)*
V_L (percentage of V_L at P_{max})	36 (6)	100 (0)*
V_T (ml/kg)	1.2 (0.2)	1.8 (0.2)*

Data reported as mean (SEM).
P_{max}, maximum pressure; P_{start}, initial pressure; V_L, lung volume; V_T, tidal volume; X_{RS}, reactance of the respiratory system.
*$P < 0.05$ vs. P_{start} (paired *t*-test).

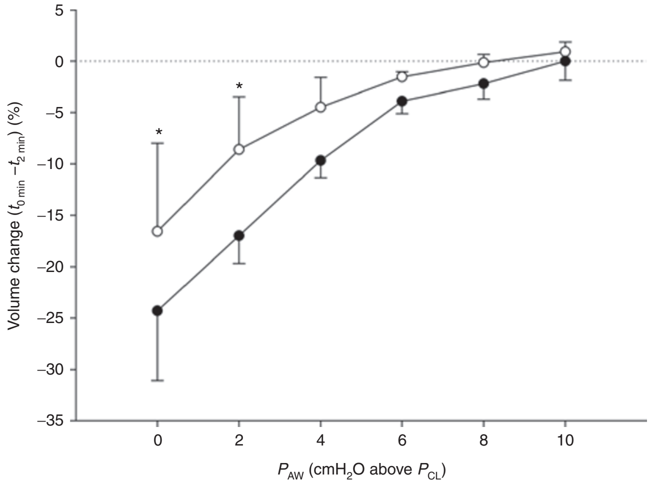

Figure 3. Dynamic changes in regional lung volume (V_L). Difference in regional end-expiratory volume recorded at t_{0min} and t_{2min} for the 2-min period at each mean airway pressure (P_{AW}) step for the ventral (open circles) and dorsal (closed circle) hemithoraces during the last five P_{AW} steps prior to closing pressure (P_{cl}) (deflation series). *Y* axis: absolute percent difference in normalized regional volume. Data expressed as mean and SEM. *$P < 0.05$ between volumes in the dorsal and ventral region (two-way ANOVA for repeated measurements with Tukey *post hoc* test).

oxygenation and X_{RS}. P_{opt} for V_L and V_T resulted in a higher Sp_{O2}/FiO_2 (fraction of inspired oxygen) than P_{opt} for oxygenation. X_{RS} and V_T at each of the P_{opt} points did not differ significantly. V_L at the P_{opt} for oxygenation was lower than at the P_{opt} for X_{RS}, V_L, and V_T (**Table 3**).

DISCUSSION

In this preterm lamb model, we used FOT during HFOV to characterize the relationship between P_{AW} and X_{RS} measured at 5 Hz. The use of oscillatory mechanics to characterize lung recruitment and to target the optimal P_{AW} was compared with oxygenation, relative V_L, and V_T. Within the recruited lung, optimal P_{AW} according to X_{RS}, as defined by its stability while at a given P_{AW}, was closely aligned with the upper corner pressure of the P_{AW}–V_L relationship, uniform recruitment, and maximal V_T. These results suggest that FOT may have use in improving the application of HFOV.

A unique feature of the present study is that the identification of the optimal pressure has been based on the stability of X_{RS} over time while at a given P_{AW}. The rationale behind this definition is that the optimal P_{AW} should be the lowest

Table 3. Ventilatory and physiological indices at the optimal pressure defined by oxygenation, reactance, end-expiratory volume, and oscillatory V_T

	At P_{opt} for oxygenation	At P_{opt} for X_{RS}	At P_{opt} for V_L	At P_{opt} for V_T
P_{AW} (cmH_2O)	13 (2)	17 (2)*	17 (2)*	16 (2)*
Sp_{O2}/FiO_2	419 (26)	425 (29)	436 (27)*	433 (28)*
X_{RS} (cmH_2O*s/l)	−34 (10)	−33 (7)	−38 (9)	−32 (7)
V_L (percentage of V_L at P_{max})	68 (7)	86 (4)*	87 (2)	81 (8)*
V_T (ml/kg)	1.8 (0.4)	1.9 (0.3)	2.0 (0.3)	2.0 (0.4)

Data reported as mean (SEM).
P_{AW}, mean airway pressure; P_{max}, maximum pressure; P_{opt}, optimal pressure; P_{start}, initial pressure; V_L, lung volume; V_T, tidal volume; X_{RS}, reactance of the respiratory system.
*$P < 0.05$ vs. P_{opt} defined using oxygenation (one-way ANOVA for repeated measurements, with Tukey *post hoc* test).

pressure able to maintain V_L after achieving full lung recruitment. Additionally, with our approach to FOT, reactance can be continuously monitored without interrupting ventilation, and thus, it is possible to track its changes over time, allowing a definition of P_{opt} that is independent from the time constants of the lung. In this way, it may be possible to identify the lowest P_{AW} that prevents derecruitment before oxygenation deteriorates.

It is well established that lung mechanics can be used to determine an optimal pressure during mechanical ventilation. However, assessing lung mechanics during HFOV is problematic, and clinically usable tools are lacking. Attempts to estimate the mechanical properties of the respiratory system from its response to the pressure oscillations delivered by the ventilator have been made in animal models (25) and, more recently, in infants using V_T as an indirect indicator of lung compliance, either via electrical impedance tomography (EIT) (26) or respiratory inductive plethysmography and pneumotachography at the airway opening (27). The similarity between the relationship of X_{RS} and V_T with pressure is not surprising, because at a given pressure amplitude, the maximum V_T that could be delivered is predominantly influenced by compliance. However, since the oscillatory periods are quite small during HFOV compared with the time constants of the lung, the actual V_T is influenced not only by compliance but also by resistance and the oscillatory frequency. Thus, the differences in V_T that we observed at 5 Hz would have been less obvious at higher oscillatory frequencies (28). Moreover, V_T does not increase linearly with compliance but asymptotically, which means that above a given compliance threshold V_T becomes largely independent from compliance, particularly at high oscillatory frequencies (29). Therefore, although the shape of the V_T and X_{RS} curves during P_{AW} maneuvers are similar, X_{RS} appears a more robust indicator of lung elastance.

X_{RS} is not yet available in the clinical setting, but measurements can be readily obtained from the response of the respiratory system to the delivered oscillatory waveform using existing monitors. This would allow real-time X_{RS} measurement to be used for titration of P_{AW} to achieve an optimal V_L

during HFOV and to identify individualized optimal ventilatory strategies.

Oxygenation is the most commonly used indicator of the volumetric response to P_{AW} (4,6,7,30), but its sensitivity to detect subtle regional volume changes is poor, it is insensitive to tissue distension and unable to define a narrow optimal point of ventilation (7,26,31). Our study suggested that oxygenation requires significant heterogeneous derecruitment before appreciable change was observed. A lag in the oxygen response to volume loss from the previously recruited lung has been described in newly born term lambs (32) and pediatric lung disease piglet models receiving HFOV (24). In contrast, changes of X_{RS} over time at a given P_{AW} were very sensitive even to partial (i.e., dorsal) V_L recruitment and derecruitment. In particular, the average difference between P_{opt} based on X_{RS} and P_{opt} based on oxygenation was about 4 cmH_2O but highly variable (range: 0–10 cmH_2O). Therefore, the P_{AW} associated with optimal V_L and mechanics cannot be simply extrapolated from P_{opt} based on oxygenation.

It is possible that the time at each P_{AW} step was too short to demonstrate a steady state in the physiological measurements. A change in X_{RS} over time indicates instability of lung mechanics at that P_{AW} and, as evident by the EIT data, increasing heterogeneity. It is possible that if we had waited for longer, all variables (including SpO_2) would have stabilized to a value indicating V_L derecruitment at a higher P_{AW}. These results highlight a potential for X_{RS} to identify that the lung is approaching derecruitment in real time at the bedside and without the need to reach suboptimal saturation levels. In the present study, we used the point of maximal curvature on the deflation limb of the pressure-V_L curve to define P_{opt} according to V_L. The point of maximal curvature identifies the P_{AW} at which there is an increase in volume loss. EIT is unable to delineate V_L loss due to a reduction in tissue distension or derecruitment. This highlights the potential benefit of a measure of lung mechanics compared with a measure of V_L in identifying a precise point of optimal P_{AW}.

FOT was assessed at 5 Hz because the use of X_{RS} at 5 Hz has been validated for the assessment of V_L recruitment (17), lung tissue distension, and P_{AW} titration (19). However, infants usually receive HFOV at higher frequencies. Therefore, performing FOT measurements required changing the prevailing frequency and also the amplitude to maintain suitable V_Ts. In the present study, EIT measurements confirmed that end-expiratory V_L did not change during the measurement, but changes in intrapulmonary pressure cannot be excluded. Mathematical modeling suggests that higher oscillatory frequencies would provide a similar P_{AW}–X_{RS} relationship but with lower sensitivity to changes occurring in the lung periphery (33). In the present study, reactance evaluated at 10 Hz identified the same P_{opt} as X_{RS}. In the future, higher oscillatory frequencies could be adopted after having confirmed the validity of the methodology *in vivo*.

This study has some limitations not already mentioned. SpO_2, X_{RS}, V_L, and V_T may be influenced by other factors than the volume state of the lung. In the present study, cuffed endotracheal tubes were used and spontaneous ventilation was suppressed to optimize the quality of the recordings. Whether similar results can be replicated in the clinical setting warrants investigation. Exogenous surfactant and antenatal corticosteroids were not used in our model. Both are known to influence lung mechanics. We contend that the relationships seen are unlikely to differ but the exact values may differ. The limitations of EIT have been well described previously (34), in particular, EIT is not commercially available for neonatal use and the different chest shape of the newborn lamb compared with the human infant may influence the regional EIT data (34). The use of Sp_{O2}/FiO_2 to report the oxygenation response to P_{AW} changes was a pragmatic decision. This variable has been used in clinical "open lung" studies in newborns (6). However, the point of optimal partial pressure of arterial oxygen may not be equal to the point of optimal Sp_{O2}/FiO_2. This may also explain why other studies found a closer correlation between the optimal pressure defined by oxygenation and by lung mechanics (22,35). Lung injury analysis was not performed in our study and it is thus unclear whether targeting an optimal point defined by X_{RS}, V_L changes or V_T is more or less lung protective than targeting oxygenation.

Conclusion

X_{RS} can be used to map lung mechanics during P_{AW} maneuvers on HFOV. In our preterm lamb model, X_{RS} defined an optimal P_{AW} significantly greater than oxygenation and similar to expiratory V_L and oscillatory V_T, making this FOT approach a potential bedside tool for optimizing P_{AW} with an open lung approach. The potential for X_{RS} stability to guide the clinical application of HFOV, and improve lung protection, warrants further investigation.

METHODS

The study was performed at the Murdoch Childrens Research Institute, Melbourne, Australia and approved by the institution's animal ethics committee. Animals were cared for in accordance with the guidelines of the National Health and Medical Research Council of Australia.

Animal Preparation

Preterm lambs at 131–132 d gestation were delivered via cesarean section from anaesthetized and sedated ewes. After delivery of the fetal head, the carotid and external jugular vessels were catheterized. Lamb was intubated with a 4.0 mm cuffed endotracheal tube (ETT). Lung liquid was drained passively for 10 s and the ETT clamped thereafter. No surfactant was administrated. The fetal chest was exteriorized and dried prior to applying 16 custom-made needle electrodes equidistant around the chest at a level 1 cm above the xiphisternum. The electrodes were connected to a GoeMF II EIT system (CareFusion, Hoechberg, Germany) and electrode placement, conductance, and signal stability were confirmed. The lamb was weighed at delivery, placed supine, and a 10-s reference EIT recording was performed (SciEIT, Carefusion, Hoechberg, Germany). The ETT was unclamped and HFOV commenced immediately (Sensormedics 3100B, Carefusion, Yorba Linda, CA). The total time between delivery and initiation of HFOV was below 90 s.

Measurements and Monitoring

Sp_{O2}, systemic blood pressure, heart rate, and body temperature were continuously monitored from birth (HP48S, Hewlett Packard, Andover, MA). The equipment for FOT consisted of pressure and flow sensors placed at the proximal end of the ETT. Airway opening pressure (P_{AO}) was measured using a pressure transducer (30 Inch-D-4V, All Sensors, Morgan Hill, CA) and flow with a custom-made mesh-type heated pneumotachograph coupled with a differential pressure transducer (1 Inch-D-4V, All Sensors). The frequency response of the pressure and flow sensors was evaluated on a bench model of immature lung and found to be flat in the range of frequencies used in this study. P_{AO} and flow signals were digitized (DAQCARD 6036-E, National Instruments, Austin, TX) at a sampling rate of 600 Hz and recorded to a laptop computer using custom-built programs for data acquisition developed using LabVIEW software (National Instruments). Changes in global and regional electrical impedance, which are related to V_L, were measured by EIT sampling at 44 Hz using the methodology we described previously (36). All parameters were measured continuously throughout mapping of the pressure–volume relationship described as follows.

Mapping of the Pressure–Volume Relationship

HFOV was commenced at a P_{AW} of 14 cmH_2O, amplitude 45 cmH_2O, frequency 10 Hz, inspiratory time 33%, and FiO_2 0.4. After a 10-min equilibration period at these baseline settings, P_{AW} was increased by 4 cmH_2O every 2 min until Sp_{O2} no longer improved, or a maximum P_{AW} (P_{max}) of 34 cmH_2O was obtained (P_{AW} values above 34 cmH_2O were associated with significant hemodynamic compromise in a pilot group). Mapping of the deflation limb then followed, initially with stepwise reduction in P_{AW} in 4 cmH_2O decrements at 2-min intervals, and then 2 cmH_2O decrements below a P_{AW} of 18 cmH_2O, until a closing pressure (P_{cl}) was identified. P_{cl} was defined as the P_{AW} at which an increase in FiO_2 by at least 0.1 was required to maintain Sp_{O2} between 88 and 94%. Immediately after (t_{0min}) and 2 min after (t_{2min}) each P_{AW} decrement, oscillatory frequency was reduced to 5 Hz and the amplitude to 20 cmH_2O (to keep the flow peaks within the working range of the flow sensor and to limit the increase in V_T as frequency was reduced) for ~10 s for the calculation of X_{RS}. X_{RS} was assessed at 5 Hz to optimize the sensitivity of the measurement to changes in peripheral mechanics (33); the duration of the measurements was kept short to prevent changes in V_L or gas exchange associated with the change in oscillatory frequency. Arterial blood gas analysis was performed at the initial P_{AW}, P_{max}, and P_{cl}. Amplitude was adjusted to achieve a partial pressure of arterial carbon dioxide of 45–55 mmHg. The amplitude was kept constant during the decremental P_{AW} series, except during X_{RS} measurement, to avoid the introduction of confounding variables. Throughout the experiment, FiO_2 was adjusted to maintain Sp_{O2} in the target range (88–94%). Lambs were euthanized humanely by intravenous pentabarbitone overdose at study completion.

Data Analysis

Sp_{O2} at t_{2min} was used as the measure of oxygenation at each pressure step and the Sp_{O2}/FiO_2 ratio (37) was calculated to compare oxygenation at different protocol steps. X_{RS} was determined from the P_{AO} and flow signals during the oscillatory cycles at t_{0min} and t_{2min} by spectral analysis using the cross-spectrum method (38). The difference between X_{RS} at t_{0min} and t_{2min} was used to evaluate the dynamics of recruitment, with a decrease in X_{RS} from t_{0min} to t_{2min} taken to indicate derecruitment (17). Alterations in V_L between t_{0min} and t_{2min} were categorized similarly.

Relative V_L was determined as the mean value of the low-pass filtered (frequency < 0.1 Hz) impedance changes measured by EIT. To better compare V_L and X_{RS}, V_L was averaged over the 10 s during each 5-Hz period, providing a single data point at t_{0min} and at t_{2min} for each P_{AW}. The EIT signal at each P_{AW} was referenced to the value immediately prior to unclamping the ETT (baseline). The cross-sectional EIT images of the lungs were divided into ventral (nongravity dependent) and dorsal (dependent) hemithoraces. To allow for intersubject comparison, the volume in each region of interest (global, dorsal, and ventral) was normalized to the volume in that region at the P_{max} for each subject (100%) and baseline (0%) (7,23). V_T (V_T) was computed by integrating the flow signal. The oscillatory volumes during the 10 s at 5 Hz were averaged for comparison with X_{RS} and V_L.

Definitions of Optimal P_{AW}

Four different definitions of P_{opt} were evaluated: (i) oxygenation-based P_{opt}, defined as P_{cl}+2 cmH_2O (4,6); (ii) X_{RS}-based P_{opt}, defined as the lowest P_{AW} that prevented a decrease in X_{RS} between t_{0min} and t_{2min}; (iii) V_L-based P_{opt}, defined as the upper corner pressure, using t_{2min} data, on the deflation limb of the V_L–P_{AW} curve (the deflation limb of the V_L–P_{AW} curve was fitted according to the model described by Venegas *et al.* (39): $V_L = a + b/(1+e^{-(P-c)/d})$. a, b, c, and d are the fitting parameters and all have a physiological correlate: a is the lower asymptote, b is the total change in V_L, c corresponds to the P_{AW} at the point of highest compliance, and d, in units of pressure, represents the distance from c of the high compliance portion of the curve. The upper corner pressure, where the function rapidly changes slope, was computed as $c+2d$ and corresponds to the intersection between the tangent to the pressure–volume curve at the point of maximal compliance ($P = c$) and the upper asymptote) (39); and (iv) V_T-based P_{opt}, defined as the lowest P_{AW} that maximized V_T at t_{2min}.

Statistical Analysis

Data were tested for normality using the Kolmogorov–Smirnov test. Differences in P_{AW} and resultant oxygenation, X_{RS}, V_L, and V_T at key points of the pressure–volume relationship were evaluated using *t*-tests or one-way ANOVA for repeated measurements as appropriate. Significance of differences between the dorsal and the ventral V_L was assessed by two-way ANOVA for repeated measurements (using P_{AW} and region as factors). The Tukey post-test was applied to all ANOVA analyses. $P < 0.05$ was considered significant. Statistical analysis was performed using SigmaStat 3.1 (Systat Software, Chicago, IL).

ACKNOWLEDGMENTS

The authors thank Shane Osterfield for his assistance in animal preparation.

STATEMENT OF FINANCIAL SUPPORT

D.G.T. is supported by a National Health and Medical Research Council Clinical Research Fellowship (Australia, grant ID 491286). D.G.T., E.J.P., and R.B. are supported by the Victorian Government Operational Infrastructure Support Program (Victoria, Australia). M.N. and M.L.V. are supported by a grant from Fondazione MBBM (Monza, Italy).

Disclosure: Politecnico di Milano University, the institution of E.Z. and R.L.D., owns a patent on the use of forced oscillation technique for the detection of lung volume recruitment/derecruitment. The other authors have no competing interests to declare.

REFERENCES

1. McCulloch PR, Forkert PG, Froese AB. Lung volume maintenance prevents lung injury during high frequency oscillatory ventilation in surfactant-deficient rabbits. Am Rev Respir Dis 1988;137:1185–92.
2. Meredith KS, deLemos RA, Coalson JJ, et al. Role of lung injury in the pathogenesis of hyaline membrane disease in premature baboons. J Appl Physiol 1989;66:2150–8.
3. Hickling KG. The pressure-volume curve is greatly modified by recruitment. A mathematical model of ARDS lungs. Am J Respir Crit Care Med 1998;158:194–202.
4. Rimensberger PC, Pache JC, McKerlie C, Frndova H, Cox PN. Lung recruitment and lung volume maintenance: a strategy for improving oxygenation and preventing lung injury during both conventional mechanical ventilation and high-frequency oscillation. Intensive Care Med 2000;26:745–55.
5. te Pas AB, Davis PG, Hooper SB, Morley CJ. From liquid to air: breathing after birth. J Pediatr 2008;152:607–11.
6. De Jaegere A, van Veenendaal MB, Michiels A, van Kaam AH. Lung recruitment using oxygenation during open lung high-frequency ventilation in preterm infants. Am J Respir Crit Care Med 2006;174:639–45.
7. Tingay DG, Mills JF, Morley CJ, Pellicano A, Dargaville PA. The deflation limb of the pressure-volume relationship in infants during high-frequency ventilation. Am J Respir Crit Care Med 2006;173:414–20.
8. Suter PM, Fairley B, Isenberg MD. Optimum end-expiratory airway pressure in patients with acute pulmonary failure. N Engl J Med 1975;292: 284–9.

9. Carvalho AR, Jandre FC, Pino AV, et al. Positive end-expiratory pressure at minimal respiratory elastance represents the best compromise between mechanical stress and lung aeration in oleic acid induced lung injury. Crit Care 2007;11:R86.
10. Suarez-Sipmann F, Böhm SH, Tusman G, et al. Use of dynamic compliance for open lung positive end-expiratory pressure titration in an experimental study. Crit Care Med 2007;35:214–21.
11. Dellacà RL, Veneroni C, Vendettuoli V, et al. Relationship between respiratory impedance and positive end-expiratory pressure in mechanically ventilated neonates. Intensive Care Med 2013;39:511–9.
12. Dorkin HL, Stark AR, Werthammer JW, Strieder DJ, Fredberg JJ, Frantz ID. Respiratory system impedance from 4 to 40 Hz in Paralyzed intubated infants with respiratory disease. J Clin Invest 1983;72:903–10.
13. Gauthier R, Beyaert C, Feillet F, Peslin R, Monin P, Marchal F. Respiratory oscillation mechanics in infants with bronchiolitis during mechanical ventilation. Pediatr Pulmonol 1998;25:18–31.
14. Sullivan KJ, Durand M, Chang HK. A forced perturbation method of assessing pulmonary mechanical function in intubated infants. Pediatr Res 1991;29:82–8.
15. Dubois AB, Brody AW, Lewis DH, Burgess BF Jr. Oscillation mechanics of lungs and chest in man. J Appl Physiol 1956;8:587–94.
16. Bellardine Black CL, Hoffman AM, Tsai LW, et al. Relationship between dynamic respiratory mechanics and disease heterogeneity in sheep lavage injury. Crit Care Med 2007;35:870–8.
17. Dellaca RL, Andersson Olerud M, Zannin E, et al. Lung recruitment assessed by total respiratory system input reactance. Intensive Care Med 2009;35:2164–72.
18. Kaczka DW, Hager DN, Hawley ML, Simon BA. Quantifying mechanical heterogeneity in canine acute lung injury: impact of mean airway pressure. Anesthesiology 2005;103:306–17.
19. Kaczka DW, Brown RH, Mitzner W. Assessment of heterogeneous airway constriction in dogs: a structure-function analysis. J Appl Physiol 2009;106:520–30.
20. Zannin E, Dellaca RL, Kostic P, et al. Optimizing positive end-expiratory pressure by oscillatory mechanics minimizes tidal recruitment and distension: an experimental study in a lavage model of lung injury. Crit Care 2012;16:R217.
21. Pillow JJ, Sly PD, Hantos Z. Monitoring of lung volume recruitment and derecruitment using oscillatory mechanics during high-frequency oscillatory ventilation in the preterm lamb. Pediatr Crit Care Med 2004;5:172–80.
22. Dellacà RL, Zannin E, Kostic P, et al. Optimisation of positive end-expiratory pressure by forced oscillation technique in a lavage model of acute lung injury. Intensive Care Med 2011;37:1021–30.
23. Kostic P, Zannin E, Andersson Olerud M, et al. Positive end-expiratory pressure optimization with forced oscillation technique reduces ventilator induced lung injury: a controlled experimental study in pigs with saline lavage lung injury. Crit Care 2011;15:R126.
24. Dellacà RL, Zannin E, Ventura ML, et al. Assessment of dynamic mechanical properties of the respiratory system during high-frequency oscillatory ventilation*. Crit Care Med 2013;41:2502–11.
25. van Genderingen HR, van Vught AJ, Duval EL, Markhorst DG, Jansen JR. Attenuation of pressure swings along the endotracheal tube is indicative of optimal distending pressure during high-frequency oscillatory ventilation in a model of acute lung injury. Pediatr Pulmonol 2002;33:429–36.
26. Miedema M, de Jongh FH, Frerichs I, van Veenendaal MB, van Kaam AH. The effect of airway pressure and oscillation amplitude on ventilation in pre-term infants. Eur Respir J 2012;40:479–84.
27. Tingay DG, Mills JF, Morley CJ, Pellicano A, Dargaville PA. Indicators of optimal lung volume during high-frequency oscillatory ventilation in infants. Crit Care Med 2013;41:237–44.
28. Pillow JJ. Tidal volume, recruitment and compliance in HFOV: same principles, different frequency. Eur Respir J 2012;40:291–3.
29. Pillow JJ, Wilkinson MH, Neil HL, Ramsden CA. *In vitro* performance characteristics of high-frequency oscillatory ventilators. Am J Respir Crit Care Med 2001;164:1019–24.
30. Lachmann B. Open up the lung and keep the lung open. Intensive Care Med 1992;18:319–21.
31. Miedema M, de Jongh FH, Frerichs I, van Veenendaal MB, van Kaam AH. Changes in lung volume and ventilation during lung recruitment in high-frequency ventilated preterm infants with respiratory distress syndrome. J Pediatr 2011;159:199–205.e2.
32. Göthberg S, Parker TA, Griebel J, Abman SH, Kinsella JP. Lung volume recruitment in lambs during high-frequency oscillatory ventilation using respiratory inductive plethysmography. Pediatr Res 2001;49:38–44.
33. Dellacà RL, Santus P, Aliverti A, et al. Detection of expiratory flow limitation in COPD using the forced oscillation technique. Eur Respir J 2004;23:232–40.
34. Leonhardt S, Lachmann B. Electrical impedance tomography: the holy grail of ventilation and perfusion monitoring? Intensive Care Med 2012;38:1917–29.
35. Goddon S, Fujino Y, Hromi JM, Kacmarek RM. Optimal mean airway pressure during high-frequency oscillation: predicted by the pressure-volume curve. Anesthesiology 2001;94:862–9.
36. Tingay DG, Copnell B, Grant CA, Dargaville PA, Dunster KR, Schibler A. The effect of endotracheal suction on regional tidal ventilation and end-expiratory lung volume. Intensive Care Med 2010;36:888–96.
37. van Genderingen HR, Versprille A, Leenhoven T, Markhorst DG, van Vught AJ, Heethaar RM. Reduction of oscillatory pressure along the endotracheal tube is indicative for maximal respiratory compliance during high-frequency oscillatory ventilation: a mathematical model study. Pediatr Pulmonol 2001;31:458–63.
38. Michaelson ED, Grassman ED, Peters WR. Pulmonary mechanics by spectral analysis of forced random noise. J Clin Invest 1975;56:1210–30.
39. Venegas JG, Harris RS, Simon BA. A comprehensive equation for the pulmonary pressure-volume curve. J Appl Physiol (1985) 1998;84:389–95.